Loughborough University

This item was submitted to Loughborough's Research Repository by the author.
Items in Figshare are protected by copyright, with all rights reserved, unless otherwise indicated.

Permeability, selectivity and distinguishing criterion of silicone membrane for supercritical CO2 and N2 in the porous media

PLEASE CITE THE PUBLISHED VERSION

https://doi.org/10.1615/JPorMedia.2019025108

PUBLISHER

Begell House

VERSION

AM (Accepted Manuscript)

PUBLISHER STATEMENT

This is the peer reviewed version of the following article: ABIDOYE, L.K. and DAS, D.B., 2019. Permeability, selectivity and distinguishing criterion of silicone membrane for supercritical CO2 and N2 in the porous media. Journal of Porous Media, 22 (8), pp.1027-1041, which has been published in final form at https://doi.org/10.1615/JPorMedia.2019025108.

LICENCE

CC BY-NC-ND 4.0

REPOSITORY RECORD

Abidoye, Luqman K., and Diganta Das. 2019. “Permeability, Selectivity and Distinguishing Criterion of Silicone Membrane for Supercritical CO2 and N2 in the Porous Media”. Loughborough University. https://hdl.handle.net/2134/12327914.v1.

Permeability, Selectivity and Distinguishing Criterion of Silicone Membrane for Supercritical CO_2 and N_2 in the Porous Media

Luqman K. Abidoye[1,2], Diganta B. Das

Chemical Engineering Department, Loughborough University, Loughborough, Leicestershire LE11 3TU, United Kingdom

[1]Current address: Department of Civil Engineering, Osun State University, PMB 4494, Osogbo, Nigeria

[2]Corresponding author; Email:kluqman2002@yahoo.co.uk; Phone: +2348142486988

Abstract

The possibility of leakage of CO_2 from the geological storage reservoir is of serious concern to stakeholders. In this work, high–pressure-temperature laboratory experiments were performed to demonstrate the application of a silicone membrane-sensor system in the monitoring of subsurface gases, especially in the leakage scenario. Mass permeation, membrane resistance to gas permeation and the gas flux across the membrane are reported for two gases, namely, CO_2 and N_2. Mass permeation of CO_2 through the membrane was more than ten times higher than that of N_2, under similar conditions. It was also found to increase with the geological depths. The gas flux remains higher for CO_2 as compared to N_2. From the results, a simple criterion for distinguishing the presence of the different gases at various geological depths was formulated based on the rate of mass permeation of gas through the membrane. Results and techniques in this work can be employed in the detection/monitoring of subsurface gas movement, especially in geological carbon sequestration.

Keywords: CO_2, geological sequestration, leakage, monitoring, silicone rubber membrane.

1. Introduction

Global warming problems arising from climate change [1] have led to the practice of geological carbon sequestration so as to limit the amount of greenhouse gases in the atmosphere [2, 46, 47]. However, the possibility of CO_2 leakage from geological carbon sequestration storage reservoir is a major concern to many stakeholders [3], [4]. This is because the leakage of CO_2 from the storage reservoir may pose serious danger to potable water aquifers that may lie along the CO_2 migration path. It also poses hazards to human and plant lives if the CO_2 finds its way to the earth's surface. Leakage of CO_2 may give rise to hazards to the marine lives if it leaks through the ocean leading to water acidification [5]. These possibilities and their adverse effects

hinder public acceptance and investors' confidence in the long term safety of the CO_2 sequestration process [4], [6].

The safety of a CO_2 storage system can be compromised as a result of gravity override and/or viscous instability in the porous media initially filled with brine [7], [8]. This causes the CO_2 to move to the top of the injection layer and bypass large quantities of brine in the storage aquifer [9–11]. Similarly, wettability alteration of the caprock can lead into the migration of the CO_2 through overlying caprock [12–14], which can lead into the leakage of CO_2. Overcoming these challenges requires the design of efficient sequestration processes, together with the effective monitoring strategies.

Existing monitoring technologies for carbon sequestration are generally built upon the measurements of physico-chemical properties of the CO_2-brine-rock system or the detectability of the reaction by-products, e.g., precipitation of carbonates in limestone-rich aquifer [15]. Electromagnetic techniques [16], infrared monitoring [17], and temperature signals [18] have been demonstrated either in the laboratory or pilot applications for subsurface monitoring of gases. Methods, such as electromagnetic techniques utilise large differences in the values of the dielectric permitivitties of CO_2 and water to establish contrasts between the original and current amounts of water and CO_2 at any time in the domain [19]. Near surface monitoring involves the analysis of near surface water, air and soil samples on a regular [20]. Numerical simulations [48, 49] have also shown the possibilities of CO_2 migration in the subsurface and its reactivity with underground minerals.

Looking at the above-listed techniques, one may draw the conclusion that a number of techniques are already proposed for the monitoring of the carbon sequestration process. However, the costs of the instruments involved in the above techniques as well as the complexity of their operations and set up are often difficult tasks. This view was shared by Zimmer et al. [21]. These authors state that the conventional techniques for porous media gas sampling are time consuming, expensive, or limited in temporal sampling density and volume. In addressing the above issues, the potential of silicone rubber as a low-cost membrane for the monitoring of the presence of gas in the porous media is examined in this paper. Silicone rubber is a widely used elastomer in a wide range of industries. It is also one of the most gas permeable elastomers [22]. The high permeability of silicone rubber to gas is due to the high flexibility of silicone-oxygen chain, which enables easy diffusion of gas molecules. This property of silicone rubber has been exploited in gas separation, drug delivery, blood oxygenation and so on [23].

Earlier, Zimmer et al. [21] and Lazik et al. [24] demonstrated the applicability of silicone rubber as a membrane in the detection of gases present in the underground and boreholes. Investigations by Zimmer et al. [21] were connected to the geological carbon sequestration project (CO_2SINK) in Ketzin, Germany. They have successfully demonstrated the detection of CO_2 front at observation wells, located at different distances to the injection well, using the gas membrane sensor that includes the silicone rubber. However, the analyses of the gases through the device rely on the mass spectrometer located on the ground surface, making the system complex and expensive to use. This however raises a question, i.e., whether or not a low-cost membrane-sensor system can be effectively applied in the monitoring of subsurface gas migration under high pressure and temperature conditions, as found in the geological carbon sequestration. As shown in the works of Cheng and Luo [25] and Zimmer et al. [21], there are many gases that can migrate in the subsurface apart from CO_2. Considering the scenario where unknown gas possibly permeates into the membrane-sensor system, how can we possibly distinguish the presence of a particular gas in the subsurface using such a system?

To respond to these questions, this work attempts to characterize the performances of flat sheet silicone rubber devised with a pressure sensor for the detection of CO_2 and N_2 in porous media. Previously, Lazik et al. [24] demonstrated the application of membrane-sensor system in the continuous monitoring of O_2 and CO_2 in a sand-filled Lysimeter. However, they used tubular membrane unlike the flat-sheet membrane used in this work. The tubular nature of the membrane used in their work seems to make the measurement of the gas concentration more tedious unlike the straightforward measurement obtained in this work. This is because the tubular membrane required sensors with tubular geometry to achieve the measurement objective. Furthermore, the authors [24] show that the subsurface gas concentration can be determined by simple measurement of physical quantities (e.g., pressure or volume) only. This principle was utilised in this work by the measurement of the pressure of the gas that permeated through the membrane into the measurement chamber of the membrane-sensor system.

In our investigations, N_2, as one of the abundant gases in the subsurface [26], is included as a model gas to create comparison for the responses of the membrane-sensor system to the presence of different gases. The characterization will be done in terms of the mass permeation of the gases through the membrane, dynamic profiles of gas fluxes across the membrane and membrane resistance to gas permeation. This work will utilize the differences in the performances of the membrane-sensor system under the influences of the different gases to establish distinguishing criterion for real-time monitoring of the gas migration in the subsurface.

The experiments involved the preparation of a porous domain with well-characterised silica sand particles. The domain boundary was made of steel cell to withstand the high pressure and

temperature conditions, applicable to geological carbon sequestration. A flat sheet silicone rubber was fitted into a steel holder together with a pressure transducer (sensor). This arrangement constitutes a membrane-sensor system, which was attached to the port at the centre of the wall of the porous domain. The experiments were designed to mimic the conditions of temperature and pressure that can be encountered by gases escaping from shallow subsurface. According to Best [27], the geobaric gradient in the continental crust is around 270 bar/km while geothermal gradients were reported to be 45 and 25^{o}C/km for the warm and cold basins, respectively [28], [29]. In this work, warm basin is considered, and the calculated conditions for different geological depths, based on the above reports, were used to design the experiments. This work serves as a follow-up to our earlier publication [30], in which multiple techniques (e.g., pH, dielectric constant, bulk electrical conductivity and membrane flux parameter) were simultaneously demonstrated for use in the monitoring of potable water aquifer contaminated by leaked CO_2 at different geological depths.

2. Materials and methods

2.1 Porous domain and materials

The porous domain used in this work was prepared using commercially available silica sand particles. The domain was used to represent a geological structure while attempts were made to mimic the real conditions corresponding to different geological depths. The silica sand (DA 14/25) was purchased from Minerals Marketing (Buxton, UK). Before use, the particles were pre-treated by washing in deionised water to remove any clay content and dried for at least 24 hours. The bulk physical properties of the silica sand (porous domain) were determined in our laboratory. Constant-head permeameter technique [31] was used to determine the permeability of the porous domain to water. The experimentally determined physical and chemical properties of the samples are listed in Tab. 1. The silicone rubber sheet (part number: RS 340-2689) used in our experiments was obtained from RS Components Ltd (Northants, UK). The sheet has an average thickness of 3mm. The gases used were high purity CO_2 and N_2, which were obtained from BOC Industrial Gases (Loughborough, UK).

2.2 Instruments and sample holder set up

The pressure of the gas that permeated through the silicone rubber membrane was measured with the HySense PR 140 pressure transducer (Hydrotechnik, GmbH, Holzheimer Strasse, Germany) with operating pressure of 0 to 100 bar. The head of the pressure transducer (PT) was fitted into locally manufactured steel holder that also holds the silicone rubber membrane in a tight position. Fig.1 shows the photograph of the sample holder filled with sand, and the steel holder, which holds the membrane and the pressure transducer (sensor). The silicone membrane was cut to the appropriate diameter to fit into the steel holder with the average

diameter of the membrane being 7.3 x 10^{-3} m while the infiltration area available for permeation is 3.8 x 10^{-3} m in diameter. The reason for the reduction in diameter for effective permeation was the metal cap on the top of the holder, which screwed down the membrane against a sintered metal disc at its base.

The sample holder is a stainless steel cell with sample height of 4cm and 10cm diameter. The configuration of the sample holder with Pressure Transducers (PT) as well as interfacing with computer system for data collection and processing was described by [30] The gap between the membrane in the steel holder and the face of the PT at the base of the steel holder provides the space for the accumulation of gas that permeates through the membrane. This space has an average volume of 1 x10^{-6} (m^3).The pressure transducers were calibrated using a portable pressure calibrator, DPI 610 (Druck Limited, Leicester, UK). Electric heaters were located at the convenient corners of the heating cabinet and the system temperature was regulated using PID temperature controller (West Control Solutions, Brighton, UK). Readings were collected every 10 s.

Fig. 2 is a schematic diagram of the experimental set up. The figure illustrates the sample holder, the positions of the PTs. Narrow steel tubes run upstream and downstream of the cell with inlet for $scCO_2$ via the upstream tube connected to the supercritical fluid pump. The outlet pipe from the bottom of the sample holder has a metering valve (Swagelok, Kings Langley, UK) to shut or control outflow from the sample holder. In all experiments, it was shut to prevent the leakage of the gas in the sample holder. Furthermore, to ensure that there is no gas leakage and that the system is at the desired pressure, a precision backpressure regulator, BPR (Equilibar, Fletcher, NC, USA) is located further down the outlet tube. The back pressure regulator is a dome loaded type using peek materials as diaphragm and was loaded with nitrogen gas (BOC Industrial Gases, Loughborough, UK) from a cylinder with appropriate gas regulator (Gas-Arc Group Ltd, Norfolk, UK). The pressure imposed on the porous domain from the supercritical fluid pump was recorded by a CR10X data logger (Campbell Scientific, Shepshed, UK).

2.3 **Experimental design**

Geological sequestration of CO_2 can take place at depth of 1km or more [3], [32]. However, migration of leaked CO_2 from the storage aquifer may occur through several geological sediments, situated at different depths that lie above the storage aquifer, before reaching the earth's surface. Based on this scenario, our experiments were designed to mimic the presence of CO_2 at the hypothetical geological depths above the storage aquifer. As pointed out in the introductory part of this work, the reports of Best [27] and Nordbotten et al. [28] were used to

180 determine the pressure and temperature, respectively at the hypothetical geological depths for
181 the experiments. Conditions at various geological depths, which were considered in this work,
182 are listed in Tab. 2. For safety concerns during our experiments, the experimental conditions
183 were chosen up to the limit of 300m depth. Fresh samples of silicone rubber membranes were
184 used at the start of each experiment. At the start of the experiment, equipment was set up by
185 placing the body of the sample holder on the bottom end piece (base cover or lid). Ports on the
186 sample holder were plugged with steel holders, which hold the PTs and the membrane. These
187 were then connected to the peripheral devices as discussed above for the automatic collection
188 and logging of data. The silica sand was poured through a metal sieve of appropriate size with
189 regular tamping to ensure uniform sand deposition. Equal amount of sand (500g) was used in
190 all experiments.
191
192 Then, the top end piece was placed in position. The weight of the top end piece compressed
193 the sand to conditions suitable for high-pressure system. After tightening all the tubing joints,
194 pressure was imposed on the BPR from the N_2 cylinder. The peek diaphragm in the BPR
195 prevents the passage of the N_2 through the downstream tubing into the porous domain. The
196 sample holder and some portions of the tubing were contained within a heating cabinet fitted
197 with electric heaters. The heaters were turned on and set at the appropriate temperature for the
198 experiment. A supercritical fluid pump (Teledyne Isco, Lincoln, USA) was filled with liquid CO_2
199 from the cylinder by opening of the valve, v-1, and setting the pump on refill mode. Following
200 this, v-1 was closed and the supercritical fluid pump was set at the experimental pressure. This
201 procedure supplied the CO_2 to the tubing from the exit of the supercritical fluid pump up to the
202 valve, v-3 (see Fig.2).
203
204 **Figure 1**
205
206 Constant pressure mode of the supercritical fluid pump was used throughout all the
207 experiments. This mode imposed constant pressure of gas on the porous domain. When the
208 temperature in the heating cabinet had reached the target condition, v-3 was opened and CO_2
209 was supplied into the sand in the sample holder. The pump being in constant pressure mode,
210 any pressure fluctuation owing to the opening of the v-3 was quickly eliminated. The experiment
211 continued for varying number of hours as convenient for the investigators. Measurements were
212 performed at different temperatures and pressures following the conditions listed in Tab. 2. In
213 addition, for each experiment, the result presented was the arithmetic average of the readings
214 from the two sensors. The silicone rubber used in this work is a non-porous flat sheet
215 membrane. Gas permeates the membrane by diffusion under the influence of the driving force,
216 e.g., the pressure difference across the membrane. Commonly, concentration gradient is
217 normally taken as the driving force in the permeation of gas through a membrane in the mixture

of gases (see, e.g., [24]). In this work, only pure gas was used in each experiment. Therefore, pressure gradient across the membrane is rightly considered to be the driving force. However, the emphasis in this work is to show the behaviour of different gases at different geological depths. As the depth is also strongly related to temperature and pressure, the emphasis on depth, in this work, can be directly related to the monitoring of gas movement in geological media at different positions. Fresh and used silicone rubber membranes scanned with the field emission gun scanning electron microscopy (FEGSEM) (LEO 1530VP, Carl Zeiss SMT, Oberkochen, Germany) are shown in Fig.3. No significant pores were detected in the membrane by the scan after the CO_2 permeation.

For the experiments involving N_2, the N_2 gas was supplied from the N_2 cylinder via the BPR. Here, v-3 was closed to prevent N_2 from entering the supercritical fluid pump. The diaphragm on the BPR was removed to provide a path for the N_2 to enter into the sand in the domain through the downstream tubing. The N_2 pressure was set on the gas regulator on top of the N_2 cylinder. All other procedures remained as defined above for the CO_2 experiments.

Figure 2

Figure 3

2.4 Calculation methods

The pressure reading at different time was used to determine the mass of the gas in the measurement chamber of the membrane-sensor system. In order to obtain real properties of the gases, Van der Waals equation was used to determine the mole of the gases. The mass of the gas was obtained from their respective mole at different time. Van der Waals equation is shown in Eq. (1):

$$[P + (n^2 a / V^2)](V - nb) = nRT \quad (1)$$

P (Pa), n (mol), V (m^3) and T (K) are the pressure, number of mole, volume and temperature, respectively, of the gas in the measurement chamber of the membrane-sensor system. R (J/mol K) is the universal gas constant, a (kg m^5/s^2mol^2) and b (m^3/mol) are constants, which fit the experiment closely to individual gas molecule. The mole, n, is obtained from equation (1) by approximating V in the term n^2a/V^2 (see, Eq. 1) using the ideal gas equation (i.e., $V=nRT/P$). After rearrangement, n is obtained as:

$$n = \frac{V(PR^2T^2 + aP^2)}{bPR^2T^2 + baP^2 + R^3T^3} \quad (2)$$

The mass, m, of the gas was obtained by multiplying the mole, n, with the molar mass of the gas.

To assess the performance of a membrane in term of the mass of gas that permeates through its matrix, Shahrabi et al. [33] describe the gas permeate flux *(J)* (kg/m^{2}hr) through the membrane as:

$$J = \frac{m}{A \cdot t} \tag{3}$$

Where *m* (g) is the total mass of the permeate at the experimental time interval, *t* (h), and *A* is the effective membrane area for permeation (m^2)

The mass transfer across a gas/membrane/gas system consists of three distinct stages. In this work, the stages are (1) mass transfer of gas across the gas boundary layer in the porous medium (2) the transfer of gas through the membrane, (3) transfer of gas across the gas boundary layer in the open space between the membrane and the pressure transducer (sensor). Each of these stages acts as a resistance to mass transfer. For a non-porous membrane, the total resistance ($1/K_T$) can be expressed in series sum of the above resistances:

$$\frac{1}{K_T} = \frac{1}{k_{g1}} + \frac{1}{k_m} + \frac{1}{k_{g2}} \tag{4}$$

Where K_T, k_{g1}, k_m, and k_{g2} are the mass transfer coefficients for overall, gas boundary in the porous medium, gas permeation through the membrane, and the gas boundary in the measurement chamber of membrane-sensor system, respectively. In this work, it can be assumed that the resistances in the gas boundary layer in the porous medium ($1/k_{g1}$) and in the open space between the membrane and the sensor ($1/k_{g2}$) are negligible. Thus, we define that $K_T \cong k_m$. This assumption is reasonable considering that the gas transfer in the porous medium was rapid because of the automatic pressure regulation from the supercritical fluid pump, which imposed constant pressure on the domain throughout the experiment. De Bo [36] similarly assumes the overall mass transfer resistance in gas/membrane/gas system is equivalent to the resistance in the non-porous membrane, like the one used in this work. The resistance to pure gas in the membrane can be determined from the Eq. (5) [37]:

$$\frac{1}{k_m} = \frac{\delta}{P} \tag{5}$$

Calculations in this work using the Eq. (2) and (3) extend over the entire duration of the experiments. This approach enables understanding of the response of the membrane–sensor system from the beginning of gas permeation through the membrane. The primary aim of this work is to understand the response of the membrane-sensor system at simulated different geological depths in the event of the CO_2 leakage from a storage reservoir and to establish a suitable distinguishing criterion with which a membrane-sensor system can be programmed to

detect different gases that permeate through a non-porous membrane in the porous media at different depths. Therefore, it is important to know the response of the membrane-sensor system at the start of the permeation, which can be used to characterise the gas leakage detection.

In all experiments, constant pressure and temperature were maintained on the porous domain. As mentioned earlier, the main driving force for the gas permeation through the membrane was the difference between the domain pressure and the pressure in the membrane-sensor system, i.e., p_1-p_0.

3. Results and discussions

In this section, the responses of the membrane-sensor system to the different imposed conditions of CO_2 and N_2 are discussed in the context of various parameters, which may affect the leakage/migration of CO_2 from a storage aquifer. As mentioned earlier, for each experiment, simultaneous double pressure readings were taken from the two pressure transducers located at the opposite sides of the centre of the porous domain. Arithmetic average of these readings was reported for each experiment in this work. Typical behavior of the membrane-sensor system is shown in Fig. 4 for CO_2 permeation into the membrane at conditions corresponding to the 250m depth (see, Tab. 2). The simultaneous readings of the two sensors (PTs) are close, having the maximum standard deviation of 4.7bar. For all experiments, the standard deviations of the simultaneous sensors' readings reduce with the decreasing depth. At 200 and 50m depths, the standard deviations are 2.8 and 0.9bar, respectively. The figure also shows that the domain pressure, which was imposed from the CO_2 pump, remained constant till the end of the experiment. In some experiments, the gas may leak through connections at the tubing joints, which seems to arise due to the high pressure of the system. This resulted in the decline of the pump and domain pressure. Results from such experiments were discarded.

Figure 4

3.1 Gas permeation in the membrane

The permeation of gas through the membrane is recorded as a change in the pressure reading of the pressure transducer. Using the Van der Waals gas equation, the pressure reading was used to determine the mass of the gas that has penetrated through the silicon rubber. The volume of the measurement chamber between the membrane and the sensor in the steel holder is known. This volume is constant and it is occupied by permeated gas under different conditions. In all experiments, no significant deformation of the membrane is visible. Therefore, the volume of the measurement chamber can be confidently assumed constant. The mass of the gas that permeates the membrane is an important parameter since it is known that the

mass is conserved. Mass of N_2 that permeated into the membrane is shown in Fig.5 at the conditions corresponding to the depths of 150 and 300m. Under these conditions, the figure shows that the time of the detection of the N_2 (i.e., start of the rise in the mass of the gas) is not significantly different for the two conditions. It takes more than an hour for any significant mass of N_2 gas to be recorded. In Fig.6, the responses of the membrane-sensor system to the presence of CO_2 at different conditions corresponding to different geological depths are shown. The rate of change of mass of CO_2 increases with depth. This can be seen as the effect of increasing pressure and temperature with depth. Comparing Figs. 5 and 6, it can be seen that under similar conditions, the level of the response of the system to the presence of CO_2 far outweighs that of N_2. Fig.7 displays this comparison clearly. At the same depth (150m), significant amount of CO_2 is detected at less than 10 minutes compared to detection of N_2, which takes more than 1 hour. This shows the quick response of the membrane-sensor system to the presence of CO_2. Observations above are similar to the findings of many authors on the high permeation rate of CO_2 in the silicone rubber membrane (see, e.g.,[21], [38], [39], [42–44]).

Figure 5

Figure 6

Figure 7

3.2 Dynamic gas flux across the membrane

The dynamic flux of gas across the membrane is calculated using Eq. (3). The dynamic gas flux across the membrane is plotted against the mass of the permeated gas in order to show the influence of the driving force on the flux profile. As mentioned earlier, the driving force is the pressure difference across the membrane. The mass of the gas in the membrane-sensor system is proportional to the pressure reading by the pressure transducer. Therefore, the plot of the gas flux against mass of permeated gas informs well about the profile of the gas flux in relation to the change in the driving force. Flux across the membrane with the permeation of N_2 is shown in Fig.8. Several stages can be discerned in the flux profile of the gas. In the first part of the curve (Fig.8, 300m depth), the gas flux increases rapidly with the mass of permeated gas. This continues until the second stage is reached where the increase in gas flux persists but at a reduced rate than the first stage. This is succeeded by the third stage, which is characterised by virtually constant flux regime. These three stages can be discerned at 300m depth in Fig. 8. In the figure, owing to the short duration of the experiment at 150m depth, only the first stage and part of the second stage are depicted.

Fig.9 shows the existence of further stage in the profile of gas flux into the membrane with CO_2. Here, we have higher permeation rate for the CO_2. This enables us to see the behavior of the flux profile more readily. Following the third stage that was characterised by virtually constant

flux of the gas into the membrane (see, Fig. 8), it is clear in Fig.9 that the fourth stage of the profile is characterised by a decline in flux for all the conditions investigated. Thus, the third stage represents the peak value of the flux following which there is gradual decline in the gas flux.

Figures 8 and 9 show that the flux of the permeated gas increases with the depth. The value of the dynamic gas flux recorded with CO_2 on the silicone rubber far outweighs that of N_2 under similar conditions. The results show that CO_2 diffuses faster through the silicone membrane than N_2. Reasons for the decline in the flux profile with the mass of the permeated gas can be explained in term of the driving force, which is defined to be the difference in pressures across the membrane. It will be recalled that the increase in the mass of the gas that permeates through the membrane actually signifies increase in the pressure of the permeated gas in the measurement chamber of the membrane-sensor system. Thus, increase in the mass of the permeated gas increases the pressure in the measurement chamber of the membrane-sensor system. Since the pressure in the porous domain remains constant throughout the experiment, the increase in the pressure on the side of the membrane-sensor system leads to the decrease in the driving force. Since the driving force reduces with increase in mass of the permeated gas, the dynamic gas flux profile continues to decline, as shown in the Figures 8 and 9. Zimmer et al. [21] calculated the CO_2 gas flux through silicone rubber and found that the flux values increase with the partial pressure of CO_2. However, their approach was different from this work as they only calculated the flux value at a steady state in gas permeation. They also show that the flux of CO_2 increases with temperature. The trends in their results conform with our findings (shown in Fig.9) for CO_2 flux values at different depths, corresponding to different pressure and temperature. The figure shows that the flux values increase with depth.

Figure 8

Figure 9

3.3 Distinguishing criterion for permeated gas

From the foregoing discussions of the results, it is possible to deduce the distinctive criterion to identify the presence of different gases that permeated through the silicone rubber membrane in the porous media, using the membrane-sensor system. For CO_2 and N_2 considered in this work, wide differences in flux and mass of gas permeated are scrutinised. Since mass is conserved irrespective of the measurement chamber volume under different temperature and pressure, the rate of change of mass of the permeated gas in the system was considered. This is very feasible since the rate of mass permeation of CO_2 through the membrane is more than 10 times higher than that of N_2 under similar conditions. Thus, the slope (i.e., mass permeation rate)

obtained from mass versus time curves at various depths can be used to obtain needed model. The model/equation obtained will be useful in the programming of the membrane-sensor system to uniquely detect the presence of a gas and possibly alert investigators to the presence of gas in the measurement chamber. The rate of permeation of the gas through the membrane was obtained from the slope of the linear equation fitted to the initial permeation stage of the mass versus time curve. For the CO_2 and N_2 at 150m depth, the mass permeation rates are 2 x 10^{-6} and 2 x 10^{-7} $kghr^{-1}$, respectively. The rate was determined from the portion of the mass permeation versus time curve, where the permeation became noticeable, i.e., at the initial stage of permeation. This stage of permeation was chosen because the response of the membrane-sensor system, at this point, is related to the early detection of the subsurface gas or leakage from the gas storage reservoir. Thus, programing the membrane-sensor system with parameters obtained at this crucial stage is advantageous for the quick detection of gas leakage in the subsurface. The mass permeation rate of CO_2 is one degree of order higher than that of N_2 at the 150m depth. The trends are similar at other corresponding depths. Thus, the presence of CO_2 can be detected if the gradient of the mass with time recorded by the system is around 2 x 10^{-6} $kghr^{-1}$ at the 150m depth. For CO_2 at the other geological depths, Fig.10 shows the variation of the mass permeation rate with depth for the two gases considered in this work. The data points are fitted to power law models, which provide the means of predicting the behavior at various depths.

Figure 10

The above method is useful in the early detection of CO_2 migration or leakage from geological reservoirs. Early detection at depth will allow for more time to tackle technical tasks before the CO_2 arrives in shallow groundwater or the earth's surface [21]. In application, alarm system can be triggered to signify the presence of CO_2, if the mass permeation rate follows the power law model provided in Fig.10. This equation can be used to program the membrane-sensor system. The analysis above shows that the CO_2 has unique mass permeation rate that is different from that of N_2. This can also be said of other gases found in the porous media. As shown, this rate is a function of depth. With the relation of the mass permeation rate to geological depth, using power law equation, this work has shown that the membrane-sensor system can be used to monitor gas leakage under different geological conditions. Thus, at any depth, the system can be applied to give unique indication of gas present. From a practical point of view, one may wonder whether membrane-sensor system can be successfully applied at deep geological sediment. The work of Lamert et al. [45] demonstrated the field measurements of electrical parameters to monitor the subsurface CO_2 movement by installing several copper electrodes at various depths up to 18.5m below the ground level around the CO_2 injection aquifer. This enables the investigators to monitor the movement of injected CO_2 in the space surrounding the injection aquifer. From this practical applications of sensors at depth by Lamert et al. [45], it is

believed that miniaturised pressure sensor with membrane can be used for monitoring at various depths. Abidoye and Bello [49] also demonstrated how a dielectric model can be employed in the subsurface monitoring of CO_2 movement. Thus, this work offers additional possibility in the monitoring for safety of geological carbon sequestration.

However, further efforts will be needed to improve on this study. For example, the miniaturised sensor can be configured with the membrane for better application. Also, future work should require similar characterization for other gases found in the subsurface, in order to obtain a broad spectrum of mass permeation rates for different gases for complete programing of membrane-sensor system. Future work should also include the field application of the membrane sensor system.

4. Conclusion

The potential of silicone rubber in the monitoring of gas migration in porous media has been demonstrated using responses of the membrane-sensor system in terms of the mass of permeated gas and the dynamic gas flux across the membrane are reported for both CO_2 and N_2. The results showed the existence of distinguishable stages of permeation for the gases. In term of the gas flux across the membrane, the first stage involves rapid rise in the flux across the membrane. This was followed by the less rapid stage of flux, where the gradient reduces and was succeeded by the stage of constant flux for a period, before the gas flux finally started to decline because of the reduction in the driving force across the membrane. The results differed considerably for the two gases with CO_2 flux occurring at higher degree of order than that of N_2, under similar conditions. The mass permeation with time for N_2 was more than ten times less than that for the CO_2. Based on the mass permeation rate for the different gases, simple criterion for distinguishing the presence of the gases at various geological depths using the membrane-sensor system was derived. The power law model was formulated for each gas to serve as the distinguishing criterion in the monitoring of the subsurface gas migration.

5. Acknowledgement

The authors acknowledge the PhD sponsorship granted by Petroleum Technology Development Fund (PTDF), Abuja, Nigeria, to one of the authors - Abidoye, L.K., during which this work was successfully executed at Loughborough University, UK. The authors are also grateful to the technologists in Department of Chemical Engineering, Loughborough University, especially Mr Tony Eyre, for their painstaking efforts in fabricating the complex experimental rig used in this work.

Symbols used

J	Mass flux of gas through the membrane	$kg(m^2hr)^{-1}$
K	Porous media permeability	m^2
k_m	Mass transfer coefficient in the membrane	ms^{-1}
kg_1	Mass transfer coefficient in the gas layer on the face of the membrane in the porous domain	ms^{-1}
kg_2	Mass transfer coefficient in the measurement chamber of the membrane-sensor system	ms^{-1}
K_T	Overall mass transfer coefficient	ms^{-1}
n	Number of mole	mol
p	Pressure of gas	bar
m	Mass of gas	kg
t	time	hr
D_p	Particle diameter	μm
PT	Pressure transducer	-
ϕ	Porosity	-
δ	Thickness of the membrane	m
V	Volume of the measurement chamber of the membrane-sensor system	m^3
T	System temperature	K
a	Van der Waals constant	$kgm^5s^{-2}mol^{-2}$
b	Van der Waals constant	m^3mol^{-1}

460

461

462 **References**

463 [1] Chandrappa, R., Gupta, S., and Kulshrestha, U.C., . Coping with climate change:
464 principles and Asian context, Springer. ISBN 978-3-642-19674-4, 2011.

465 [2] Ward, S.E., Ostle, N.J., Oakley, S., Quirk, H., Henrys, P.A., and Bardgett, R.D.
466 "Warming effects on greenhouse gas fluxes in peatlands are modulated by vegetation
467 composition," *Ecology letters*, vol. 16, no. 10, pp. 1285–1293, 2013.

468 [3] Abidoye, L.K., Das, D.B. and Khudaida, K. Geological carbon sequestration in the
469 context of two-phase flow in porous media: A review. Critical Reviews in Environmental Science
470 and Technology, 45(11), pp. 1105-1147 DOI: 1080/10643389.2014.924184 2014.

471 [4] Itaoka, K., Saito, A. and Akai, M.. Public acceptance of CO_2 capture and storage
472 technology: a survey of public opinion to explore influential factors. In Proceedings of the
473 7. international conference on greenhouse gas control technologies, Vancouver, BC
474 (Canada); 5-9 Sep 2004

475 [5] Klapper, R., Widdicombe, S. and Reitz, A. "ECO2 Briefing Paper No. 2: Potential impacts
476 of CO_2 leakage from sub-surface storage on seabed biology," 2013.

477 [6] Krause, R.M., Carley, S. R., Warren, D. C., Rupp, J. A., and Graham, J. D.. Not in (or
478 Under) My Backyard: Geographic proximity and public acceptance of carbon capture and
479 storage facilities. Risk Analysis, 34(3), pp.529–540., 2014

[7] Taku Ide, S., Jessen, K. and Orr Jr, F.M. "Storage of CO_2 in saline aquifers: Effects of gravity, viscous, and capillary forces on amount and timing of trapping," *International Journal of Greenhouse Gas Control*, vol. 1, no. 4, pp. 481–491, 2007.

[8] Berg, S and Ott, H. "Stability of CO_2–brine immiscible displacement," *International Journal of Greenhouse Gas Control*, vol. 11, pp. 188–203, Nov. 2012.

[9] Tao, Q and Bryant, S.L. "Well permeability estimation and CO2 leakage rates," *International Journal of Greenhouse Gas Control*, vol. 22, pp. 77–87, Mar. 2014.

[10] Gasda, S.E., Nordbotten, J.M. and Celia, M.A. "Vertical equilibrium with sub-scale analytical methods for geological CO_2 sequestration," *Computational Geosciences*, vol. 13, no. 4, pp. 469–481, 2009.

[11] Saripalli, K.P., Mcgrail, B.P. and White, M.D. "Modeling the sequestration of CO2 in deep geological formations," in *First National Conference on Carbon Sequestration*, no. 509, pp. 1–19, 2001

[12] Saraji, S., Goual, L., Piri, M. and Plancher, H, "Wettability of supercritical carbon dioxide/water/quartz systems: simultaneous measurement of contact angle and interfacial tension at reservoir conditions.," *Langmuir : the ACS journal of surfaces and colloids*, vol. 29, no. 23, pp. 6856–6866, Jun. 2013.

[13] Al-Garni , M.T. and Al-Anazi, B.D. "Investigation of wettability effects on capillary pressure, and irreducible saturation for Saudi crude oils, using rock centrifuge," *Oil and Gas Business*, vol. 2008, no 2, 2008.

[14] Chiquet, P., Broseta, D. and Thibeau, S. "Wettability alteration of caprock minerals by carbon dioxide," *Geofluids*, vol. 7, no. 2, pp. 112–122, May 2007.

[15] Espinoza, D.N., Kim, S.H., and Santamarina, J.C. "CO_2 geological storage — Geotechnical implications," *KSCE Journal of Civil Engineering*, vol. 15, no. 4, pp. 707–719, Apr. 2011.

[16] Nakatsuka,Y., Xue, Z., Garcia, H. and Matsuoka, T. "Experimental study on CO_2 monitoring and quantification of stored CO_2 in saline formations using resistivity measurements," *International Journal of Greenhouse Gas Control*, vol. 4, no. 2, pp. 209–216, 2010.

[17] Charpentier, F. Bureau, B. Troles, J. Boussard-Plédel, C. Michel-Le Pierrès, K., Smektala, F. and Adam, J.-L. "Infrared monitoring of underground CO_2 storage using chalcogenide glass fibers," *Optical Materials*, vol. 31, no. 3, pp. 496–500, 2009.

[18] Bielinski, A., Kopp, A., Schütt, H., and Class, H. "Monitoring of CO_2 plumes during storage in geological formations using temperature signals: Numerical investigation," *International Journal of Greenhouse Gas Control*, vol. 2, no. 3, pp. 319–328, 2008.

[19] Vilamajó, E., Queralt, P., Ledo, J. and Marcuello, A. "Feasibility of Monitoring the Hontom{í}n (Burgos, Spain) CO_2 Storage Site Using a Deep EM Source," *Surveys in Geophysics*, vol. 34, no. 4, pp. 441–461, 2013.

[20] Spangler, L.H., Dobeck, L.M. Repasky, K.S. Nehrir, A.R. Humphries, S.D., Barr, J.L., Keith, C.J., Shaw, J.A., Rouse, J.H. and Cunningham, A.B. "A shallow subsurface controlled release facility in Bozeman, Montana, USA, for testing near surface CO_2

detection techniques and transport models," *Environmental Earth Sciences*, vol. 60, no. 2, pp. 227–239, 2010.

[21] Zimmer, M., Erzinger, J. and Kujawa, C. "The gas membrane sensor (GMS): A new method for gas measurements in deep boreholes applied at the CO2SINK site," *International Journal of Greenhouse Gas Control*, vol. 5, no. 4, pp. 995–1001, Jul. 2011.

[22] Zhang, H. and Cloud, A. "The permeability characteristics of silicone rubber," in *Proceedings of the 2006 SAMPE Fall Technical Conference" Global Advances in Materials and Process Engineering", Coatings and Sealants Section*, 2006.

[23] Barnes,A.C., Dejuan Jr, E., Humayun, M., Shelley, T. and Varner, S.E. "Devices for intraocular drug delivery." Google Patents, 2012.

[24] Lazik, D., Ebert, S., Leuthold, M. Hagenau, J. and Geistlinger, H. "Membrane Based Measurement Technology for in situ Monitoring of Gases in Soil.," *Sensors (Basel, Switzerland)*, vol. 9, no. 2, pp. 756–67, Jan. 2009.

[25] Cheng, J. and Luo, Y. "Modeling Atmosphere Composition and Determining Explosibility in a Sealed Coal Mine Volume," *Archives of Mining Sciences*, vol. 59, no. 1, pp. 25–40, 2014.

[26] Bednarek, A., Szklarek, S. and Zalewski, M. "Nitrogen pollution removal from areas of intensive farming—comparison of various denitrification biotechnologies," *Ecohydrology & Hydrobiology*, vol. 14, no. 2, pp. 132–141, 2014.

[27] Best, M.G. *Igneous and Metamorphic Petrology*. John Wiley & Sons, 2013.

[28] Nordbotten, J.M., Celia, M.A. and Bachu, S. "Analytical solutions for leakage rates through abandoned wells," *Water Resources Research*, vol. 40(4), Apr. 2004. DOI:10.1029/2003WR002997

[29] Das, D.B., Gill, B.S., Abidoye, L.K. and Khudaida, K.J. "A numerical study of dynamic capillary pressure effect for supercritical carbon dioxide-water flow in porous domain," *AIChE Journal*, DOI 10.1002/aic.14577 (in press). 2014.

[30] Abidoye, L.K. and Das, D.B. pH, Geoelectrical and Membrane Flux Parameters for the Monitoring of Water-Saturated Silicate and Carbonate Porous Media Contaminated by CO2. Chemical Engineering Journal, 262, pp. 1208–1217, 2015.. [31] Bear, J. *Dynamics of fluids in porous media*. Courier Dover Publications, 2013.

[32] Hosseini, S.A., Lashgari, H., Choi, J.W., Nicot, J.-P, Lu, J. and Hovorka, S.D. "Static and dynamic reservoir modeling for geological CO_2 sequestration at Cranfield, Mississippi, U.S.A.," *International Journal of Greenhouse Gas Control*, vol. 18, pp. 449–462, Oct. 2013.

[33] Salehi Shahrabi, S., Mortaheb, H.R., Barzin, J. and Ehsani, M.R. "Pervaporative performance of a PDMS/blended PES composite membrane for removal of toluene from water," *Desalination*, vol. 287, pp. 281–289, Feb. 2012.

[34] Baker, R.W. *Membrane Technology and Applications*, 3rd ed. John Wiley & Sons, , p. 592., 2012.

[35] Van Amerongen, G.J. "Diffusion in elastomers," *Rubber Chemistry and Technology*, vol. 37, no. 5, pp. 1065–1152, 1964.

562 [36] De Bo, I. “Investigation of the permeability and selectivity of gases and volatile organic
563 compounds for polydimethylsiloxane membranes,” *Journal of Membrane Science*, vol.
564 215, no. 1–2, pp. 303–319, Apr. 2003.

565 [37] Ozturk, B. and Hughes, R. “Evaluation of mass transfer characteristics of non-porous
566 and microporous membrane contactors for the removal of CO_2,” *Chemical Engineering*
567 *Journal*, vol. 195–196, pp. 122–131, Jul. 2012.

568 [38] Kesson, J. “The diffusion of gases through a silicon rubber membrane and its application
569 to an in-line carbonation meter. MBAA Technical Quarterly 21 (3), 143–146.,” *MBAA*
570 *Technical Quarterly*, vol. 21, no. 3, pp. 143–146, 1984.

571 [39] Staude, E. “Membranen und Membranprozesse,” *VCH Weinheim*, p. 325 pp., 1992.

572 [40] Praveen, J.H.A., Mason, L.W., and Way, J.D. “Characterization of silicon rubber
573 membrane materials at low temperature and low pressure conditions” *Journal of*
574 *Membrane Science*, vol. 272, pp. 125–136, 2006.

575 [41] Merkel, T.C., Gupta, R.P., Turk, B.S. and Freeman,B.D. “Mixed-gas permeation of
576 syngas components in poly (dimethylsiloxane) and poly (1-trimethylsilyl-1-propyne) at
577 elevated temperatures,” *Journal of Membrane Science*, vol. 191, no. 1, pp. 85–94, 2001.

578 [42] Egli, S., Ruf, A. and Buck, A. “Gastrennung mittels Membranen. Ein {Ü}berblick,” *Swiss*
579 *Chem*, vol. 6, no. 9, pp. 89–122, 1984.

580 [43] Praveen, J.H.A., Mason, L.W., and Way, J.D. “Characterization of silicon rubber
581 membrane materials at low temperature and low pressure conditions,” *Journal of*
582 *Membrane Science*, vol. 272, pp. 125–136, 2006.

583 [44] Merkel, T.C., Gupta, R.P. Turk, B.S. and Freeman, B.D. “Mixed-gas permeation of
584 syngas components in poly (dimethylsiloxane) and poly (1-trimethylsilyl-1-propyne) at
585 elevated temperatures,” *Journal of Membrane Science*, vol. 191, no. 1, pp. 85–94, 2001.

586 [45] Lamert, H., Geistlinger, H., Werban, U., Schütze, C., Peter, A., Hornbruch, G., Schulz,
587 A., Pohlert, M., Kalia, S., Beyer, M. and others, “Feasibility of geoelectrical monitoring
588 and multiphase modeling for process understanding of gaseous CO2 injection into a
589 shallow aquifer,” *Environmental Earth Sciences*, vol. 67, no. 2, pp. 447–462, 2012.

590 [46] Ampomah, W., Balch, R., Grigg, R.B., Cather, M., Gragg, E., Will, R.A., White, M.,
591 Moodie, N. and Dai, Z. Performance assessment of CO2-enhanced oil recovery and
592 storage in the Morrow reservoir. Geomechanics and Geophysics for Geo-Energy and
593 Geo-Resources, 3(3), pp.245-263, 2017.

594 [47] Rathnaweera, T.D., Ranjith, P.G. and Perera, M.S.A. Experimental investigation of
595 geochemical and mineralogical effects of CO 2 sequestration on flow characteristics of
596 reservoir rock in deep saline aquifers. Scientific reports, 6, p.19362., 2016.

597 [48] Xiao, T. Dai, Z., McPherson, B., Viswanathan , H. and Jia, W. Reactive transport
598 modeling of arsenic mobilization in shallow groundwater: impacts of CO2 and brine
599 leakage. Geomechanics and Geophysics for Geo-Energy and Geo-Resources, 3(3),
600 pp.339-350, 2017.

601 [49] Abidoye, L.K. and Bello, A.A. Simple dielectric mixing model in the monitoring of CO2
602 leakage from geological storage aquifer. Accepted in Geophysical Journal International,
603 208(3), pp. 1787-1795, 2017. doi: 10.1093/gji/ggw495.

604

605

606

607

608

609

610

611

612

613

614 **Tab. 1**: Bulk properties of silica sand used in our experiments

Permeability, K (m^2)	3.65×10^{-10}
Porosity, ϕ	0.37
Particle Density (kg/m^3)	2740
Average Particle Diameter, D_p (μm)	946.1
SiO_2 content (%)	99[a]

615 [a] www.sibelco.co.uk (accessed May 2014)

616

617

618

619

620

Tab. 2: List of Experimental Conditions and State of CO_2

Depth (m)	**Domain Temperature (ºC)**	**Domain/Injection Pressure (bar)**
50	22.25	13.5
150	26.75	40.5
200	29	54
250	31.25	67.5

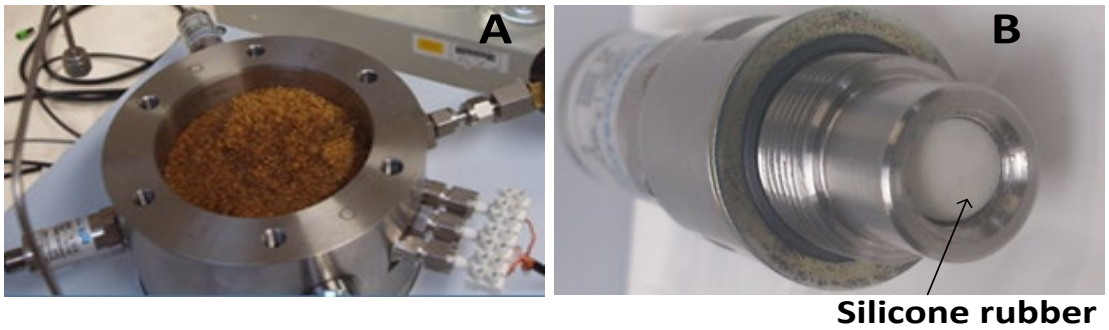
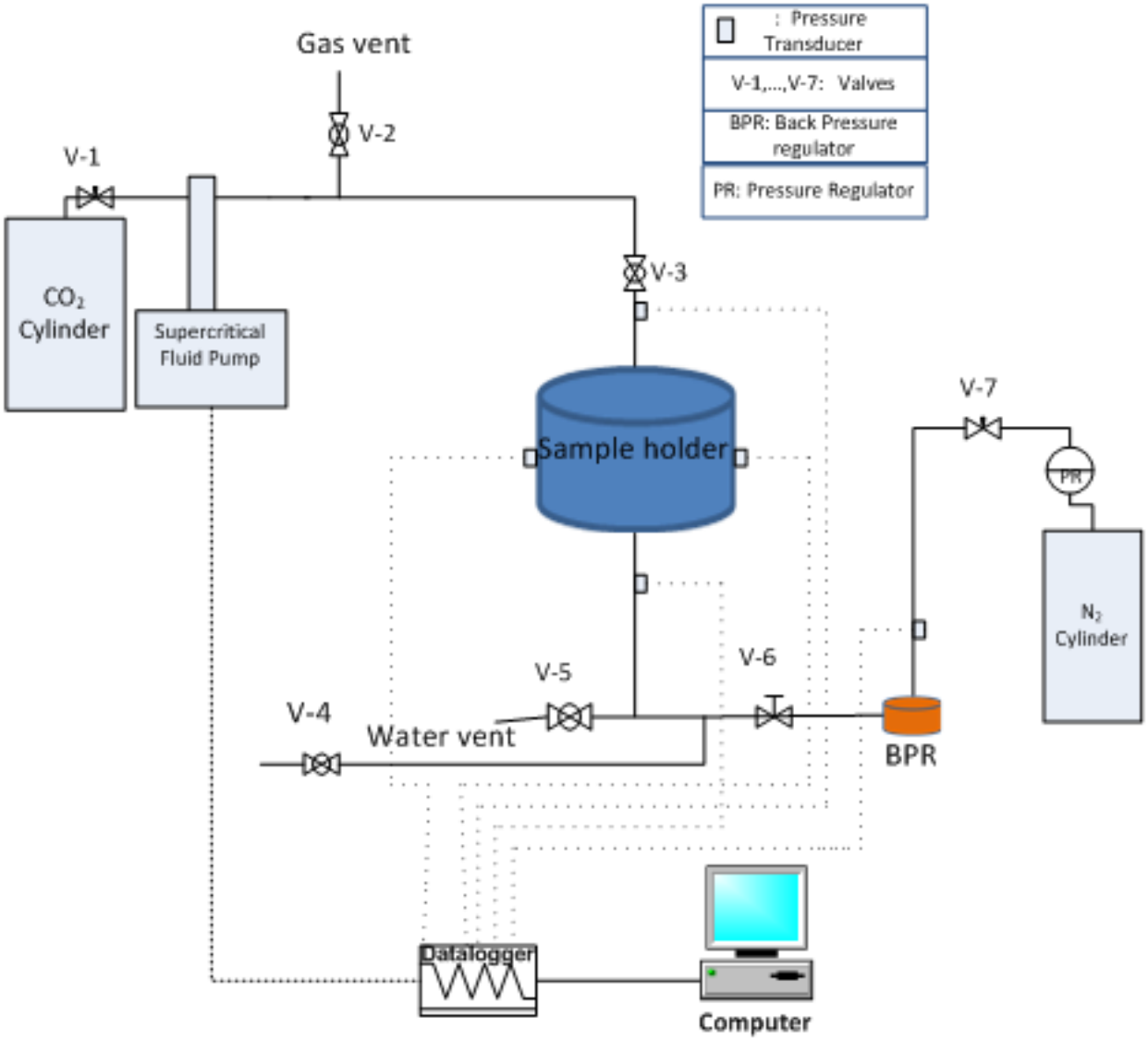


Fig 1:



654

655 Fig. 2

656

657

658

659

660

661

662

663

664

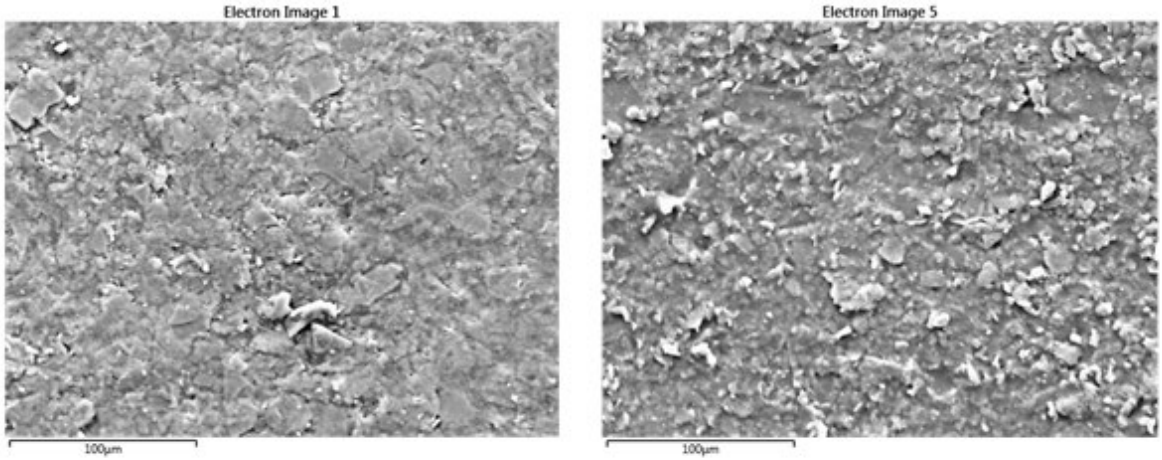


Fig. 3

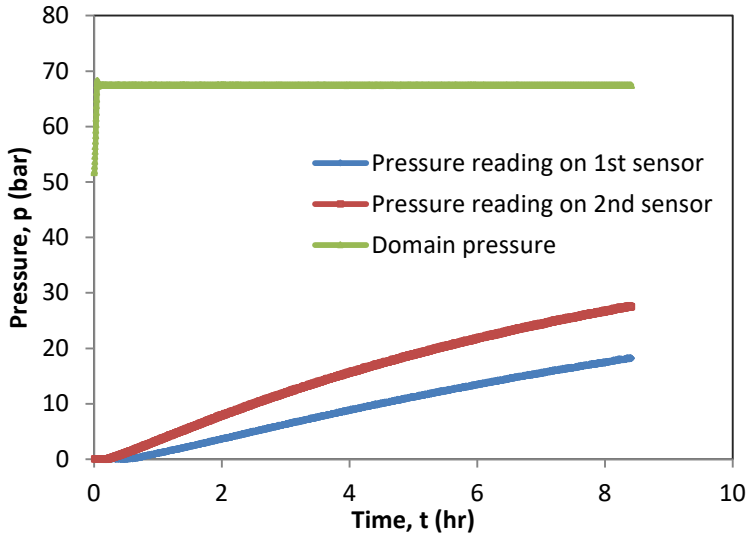

80
70
60
50
40
30
20
10
0
Pressure, p (bar)
0
2
4
6
8
10
Time, t (hr)
Pressure reading on 1st sensor
Pressure reading on 2nd sensor
Domain pressure

Fig. 4

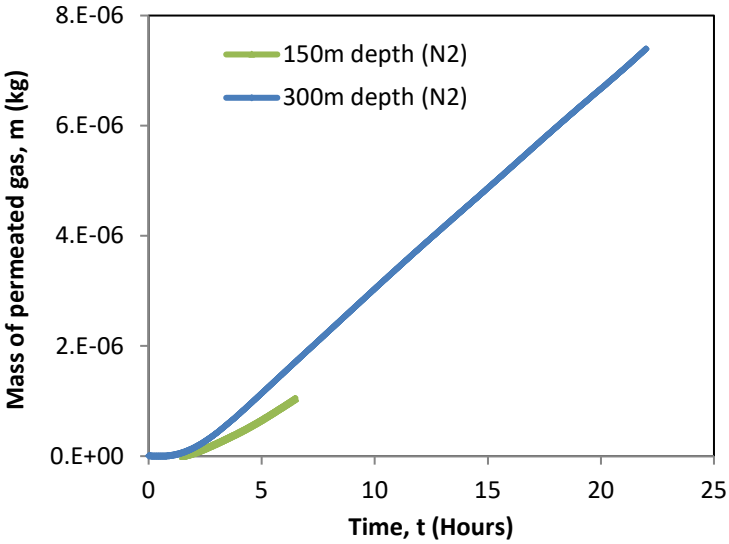

8.E-06
6.E-06
4.E-06
2.E-06
0.E+00
Mass of permeated gas, m (kg)
150m depth (N2)
300m depth (N2)
0
5
10
15
20
25
Time, t (Hours)

Fig. 5

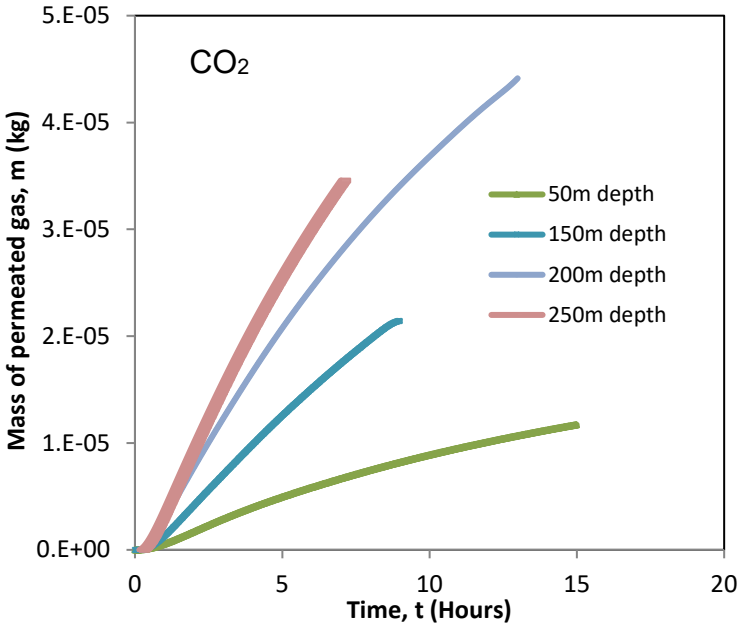

CO2
Mass of permeated gas, m (kg)
5.E-05
4.E-05
3.E-05
2.E-05
1.E-05
0.E+00
0
5
10
15
20
Time, t (Hours)
50m depth
150m depth
200m depth
250m depth

Fig. 6

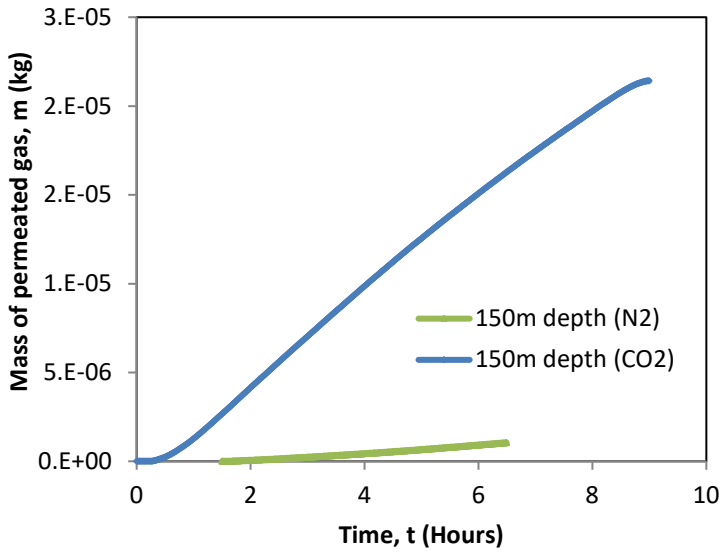

3.E-05
2.E-05
2.E-05
1.E-05
5.E-06
0.E+00
Mass of permeated gas, m (kg)
0
2
4
6
8
10
Time, t (Hours)
150m depth (N2)
150m depth (CO2)

Fig. 7

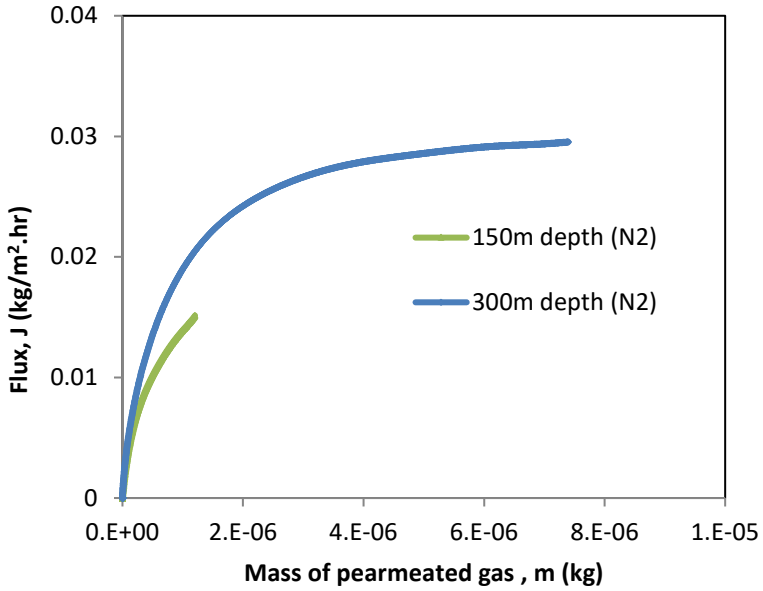

0.04
0.03
0.02
0.01
0
Flux, J (kg/m².hr)
150m depth (N2)
300m depth (N2)
0.E+00
2.E-06
4.E-06
6.E-06
8.E-06
1.E-05
Mass of pearmeated gas , m (kg)

Fig. 8

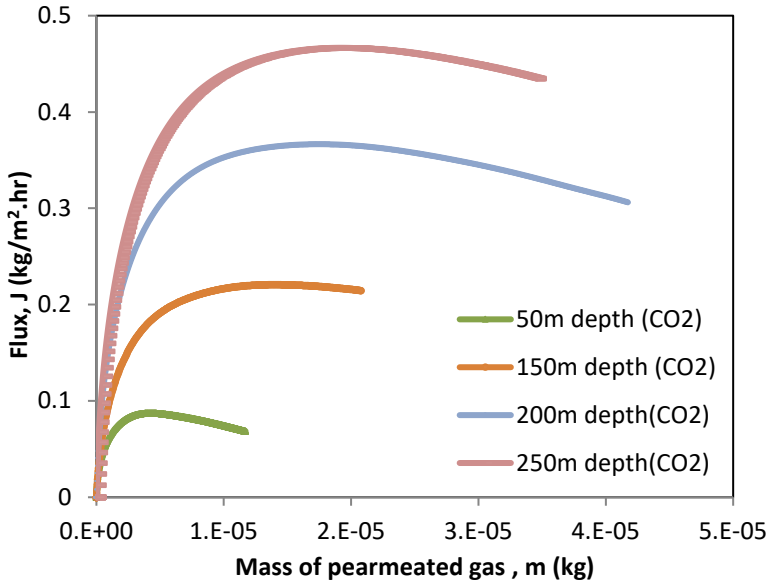

0.5
0.4
0.3
0.2
0.1
0
Flux, J (kg/m2.hr)
0.E+00
1.E-05
2.E-05
3.E-05
4.E-05
5.E-05
Mass of pearmeated gas , m (kg)
50m depth (CO2)
150m depth (CO2)
200m depth(CO2)
250m depth(CO2)

Fig. 9

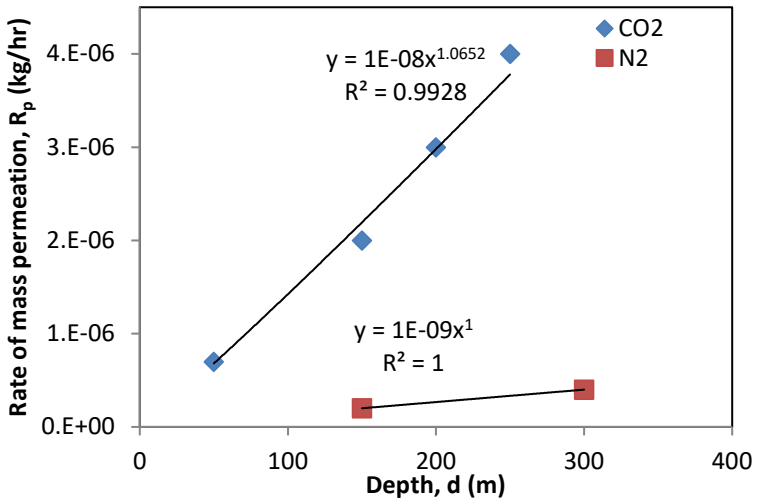

Rate of mass permeation, R_p (kg/hr)
4.E-06
3.E-06
2.E-06
1.E-06
0.E+00
0
100
200
300
400
Depth, d (m)
CO2
N2
y = 1E-08x^1.0652
R² = 0.9928
y = 1E-09x^1
R² = 1

Fig. 10

821

822

823

Fig.1: Photographs of (A) The sample holder showing silica sand and pressure transducer (B) Membrane-sensor system: Steel holder holds the pressure transducer at the rear and the silicone rubber sheet at the front (metal cap not shown). Sample holder size: internal diameter=10cm, sample height=4cm

Fig.2: High-pressure experimental set-up for the investigation of gas migration in the porous media using membrane-sensor system

Fig.3: Scans of (A) Fresh (B) Used (experiment at 67.5 bar, 31.25^{o}C, i.e., 200m depth) silicone rubber membrane using FEGSEM (LEO 1530VP, Carl Zeiss SMT, Oberkochen, Germany)

Fig.4: Simultaneous responses of the two pressure transducers to the CO_2 gas that permeated through the membrane at imposed conditions corresponding to 250m depth. Plots identification for black and white print: Top plot (domain pressure), Middle plot (2nd sensor), Bottom plot (1st sensor)

Fig.5: Mass of permeated gas (N_2) under conditions that mimic different depths. Upper plot(300m depth), lower plot (150m depth)

Fig.6: Mass of permeated gas (CO_2) through the membrane under conditions that mimic different depths. Uppermost (250m depth), 2nd plot (200m), 3rd plot (150m), lowermost plot(50m depth)

Fig.7: Mass of permeated gases (CO_2 and N_2) through the membrane under similar conditions. Upper plot (CO2), lower plot (N2)

Fig.8: Change in the flux of permeated gas (N_2) under conditions that mimic different depths. Upper plot (300m depth), lower plot (150m depth)

Fig.9: Change in the flux of permeated gas (CO_2) under conditions that mimic different depths. . Uppermost (250m depth), 2nd plot (200m), 3rd plot (150m), lowermost plot(50m depth)

855

856

857 **Fig.10:** Models of mass permeation rate for different gases at different geological depths for
858 application in the distinction of the presence of the different gases in the porous medium.

859

860

861